Electronic Supplementary Material (ESI) for Analyst.

Supporting Information

Novel Dual Response Ratiometric Fluorescence Probe for Determination of H_2O_2 and Glucose *via* Etching of Silver Nanoparticles

Hongzhi Lu[a], Chunwei Yu [b], Shuai Quan[c], Shoufang Xu[c]*,

[a] School of Chemistry and Chemical Engineering, Linyi University, Linyi 276005, China

[b] Laboratory of Environmental Monitoring, School of Tropical and Laboratory Medicine, Hainan Medical University, Haikou 571101, China

[c] School of Materials Science and Engineering, Linyi University, Linyi 276005, China

* Corresponding author, E-mail shfxu1981@163.com

1. **The interaction of CDs, Ag NPs, silver ions and H_2O_2**

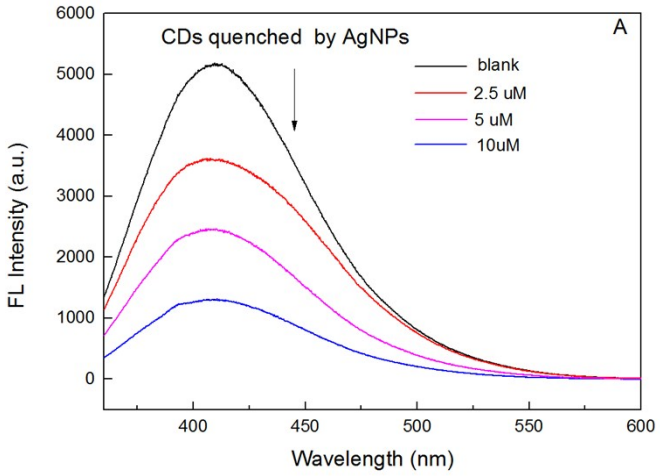

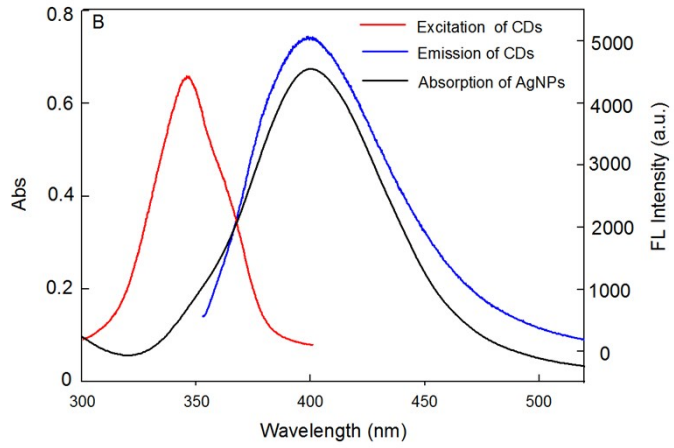

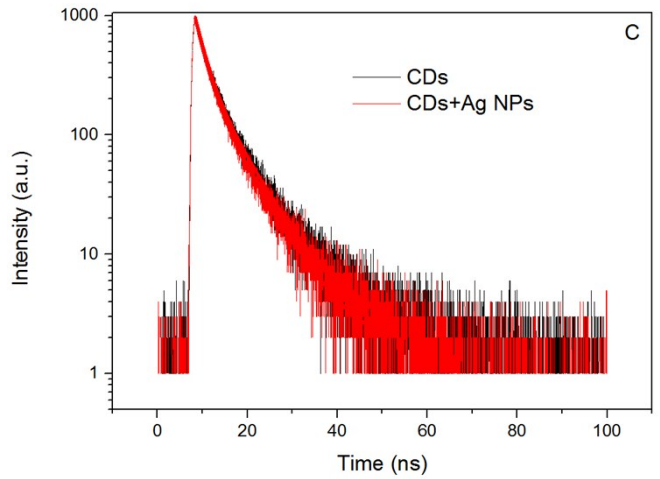

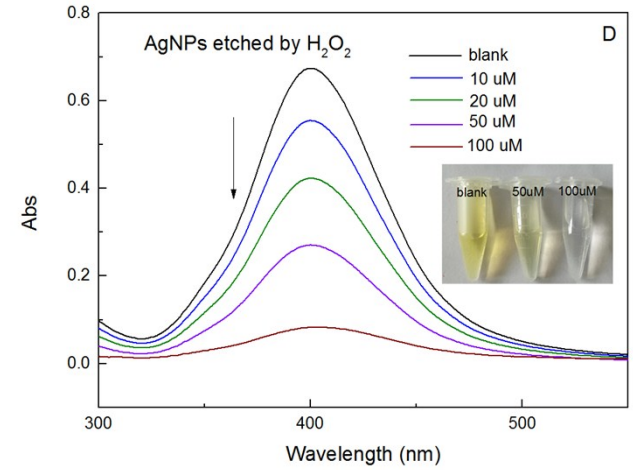
D
AgNPs etched by H_2O_2
blank
10 uM
20 uM
50 uM
100 uM
blank
50uM
100uM
Abs
Wavelength (nm)

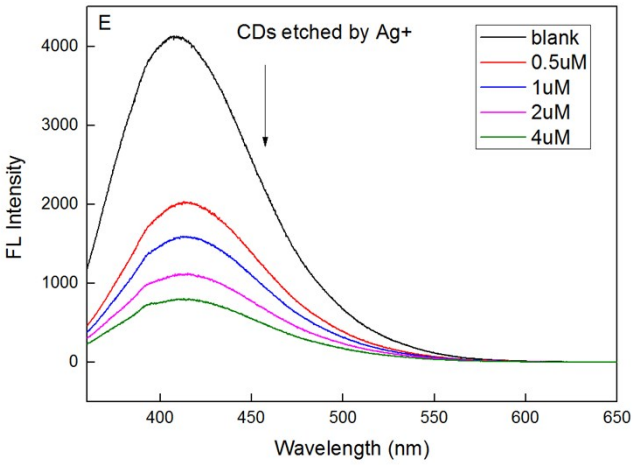
E
CDs etched by Ag+
blank
0.5uM
1uM
2uM
4uM
FL Intensity
Wavelength (nm)

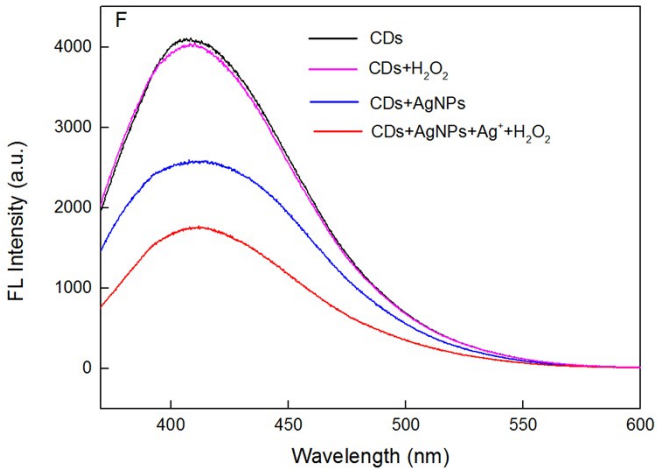
F
CDs
CDs+H_2O_2
CDs+AgNPs
CDs+AgNPs+Ag^++H_2O_2
FL Intensity (a.u.)
Wavelength (nm)

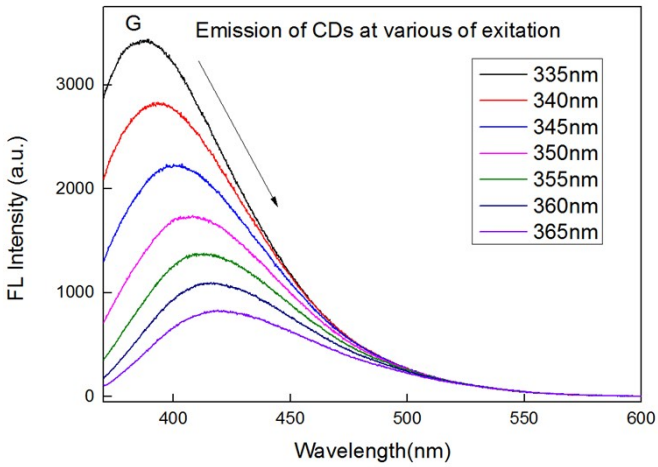

Figure S 1. (A) Fluorescence titrations of the CDs (10 μg·mL^{-1}) with AgNP from 2.5 to 10μM.

(B) UV−vis absorption spectra of AgNPs and FL excitation and FL emission spectra of CDs.

(C) The fluorescence lifetime of CDs before and after addition of Ag NPs.

(D) UV−vis absorption spectra of AgNPs in the presence of H_2O_2 from 0 to 100 μmol L^{-1}.

(E) Fluorescence titrations of the CDs (10 μg·mL^{-1}) with Ag^+ from 0.5 to 4.0 μM.

(F) The effect of H_2O_2, AgNPs, and Ag^+ on the FL intensity of CDs.

(G) FL emission spectra of the CDs recorded at various excitation wavelengths in the range of 335−365 nm.

2. The interaction of QDs, Ag NPs, silver ions and H_2O_2

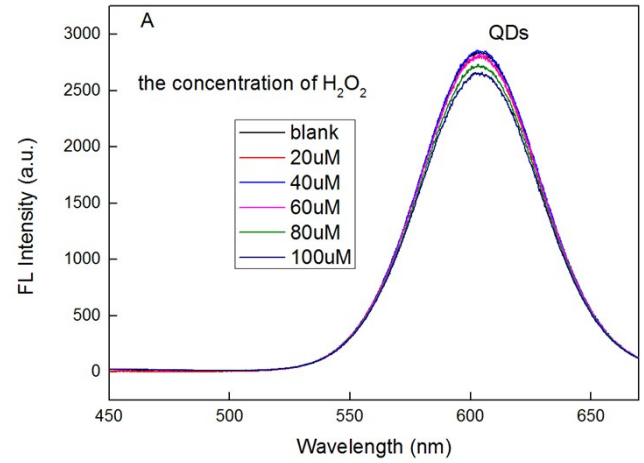

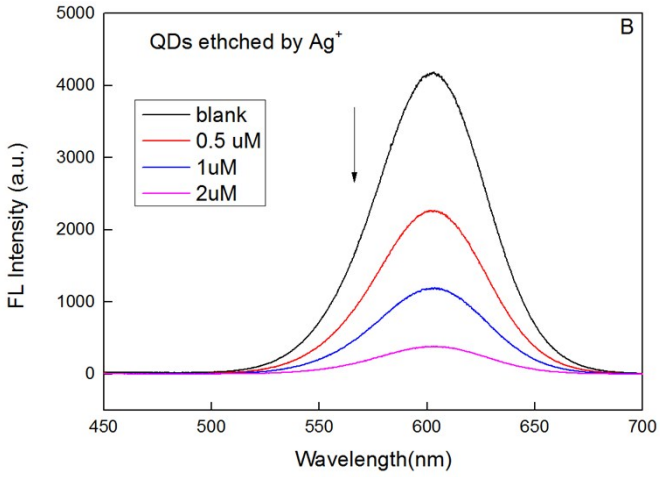

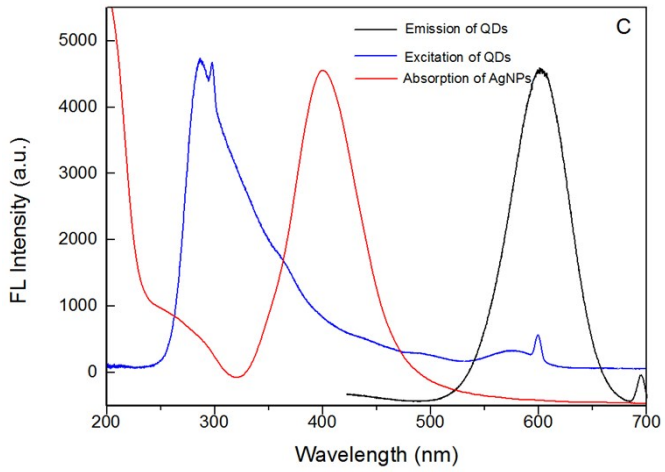

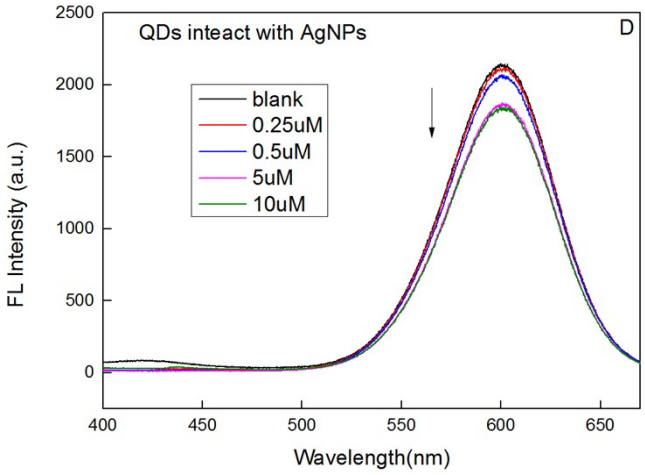

Figure S 2. (A) The effect of H_2O_2 on the FL intensity of QDs.

(B) Fluorescence titrations of the QDs (20 μg·mL^{-1}) with Ag^+ from 0.5 to 2.0 μM.

(C) UV−vis absorption spectra of AgNPs and FL excitation and FL emission spectra of QDs.

(D) Fluorescence titrations of the QDs (10 μg·mL^{-1}) with AgNP from 0.25 to 10 μM.

3. TEM images of samples.

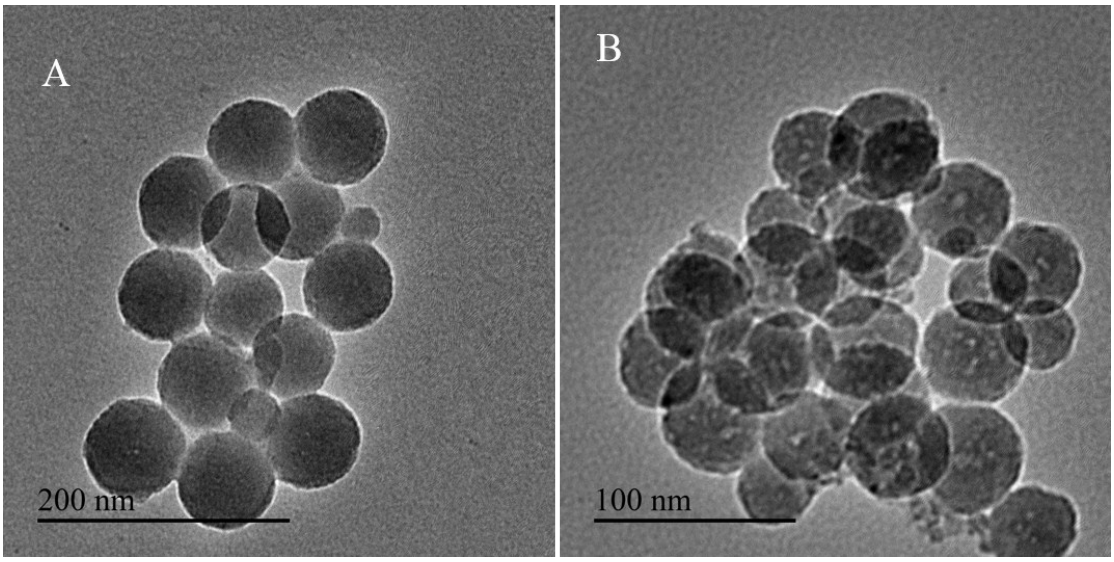

Figure S3 The TEM images of CDs@SiO_2 (A) and CDs@SiO_2@QDs (B).

4. The stability of D-RFP

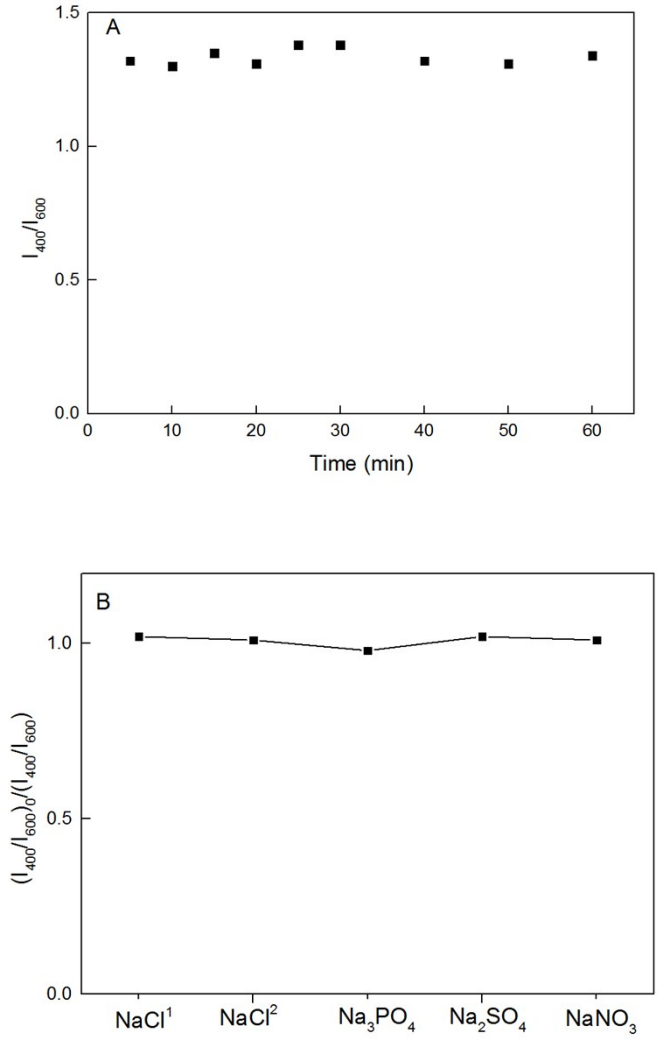

Figure S4 (A) Stability of the FL intensity of the ratiometric. The change of the relative intensity is not significant (< 5%) in 1h.

(B) The tolerance of the D-RFP to various anions (sodium salt) in phosphate buffer (pH=7.4, 10 mM). The fluorescence intensity ratio maintains nearly stable before and after the addition of various anions (10 mM) ($NaCl^1$ 10 mM, $NaCl^2$ 20 mM).

$(I_{400}/I_{600})_0$ and (I_{400}/I_{600}) represents the ratiometric signal before and after the anion addition, respectively.

5. Optimization of reaction conditions for H_2O_2 detection

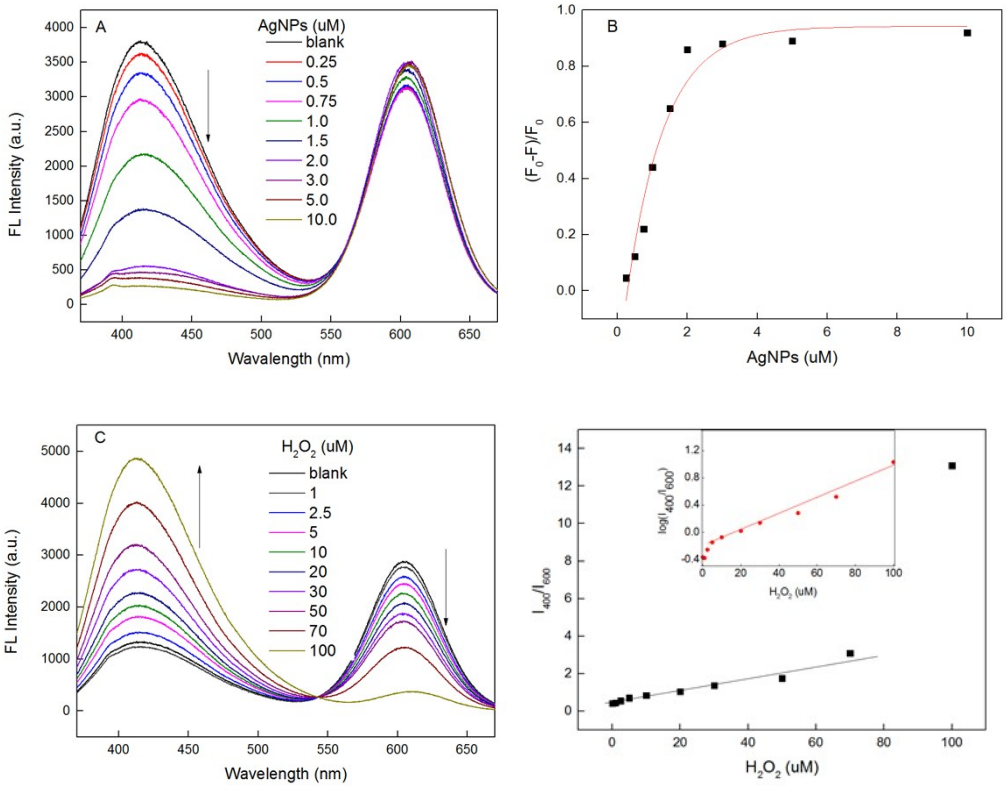

Figure S5 (A) Fluorescence titrations of the D-RFP (50 μg·mL^{-1}) with Ag NPs from 0.25 to 10 μM.

(B) Quenching efficiency of D-RFP (50 μg·mL^{-1}) versus the concentration Ag NPs at 400 nm.

(C) Fluorescence response of D-RFP and Ag NPs (50 μg.mL^{-1} and 3 μM, respectively) in the presence of different concentration of H_2O_2.

(D) The relationship between ratio of fluorescence intensity of the D-RFP in (C) versus concentration of H_2O_2.

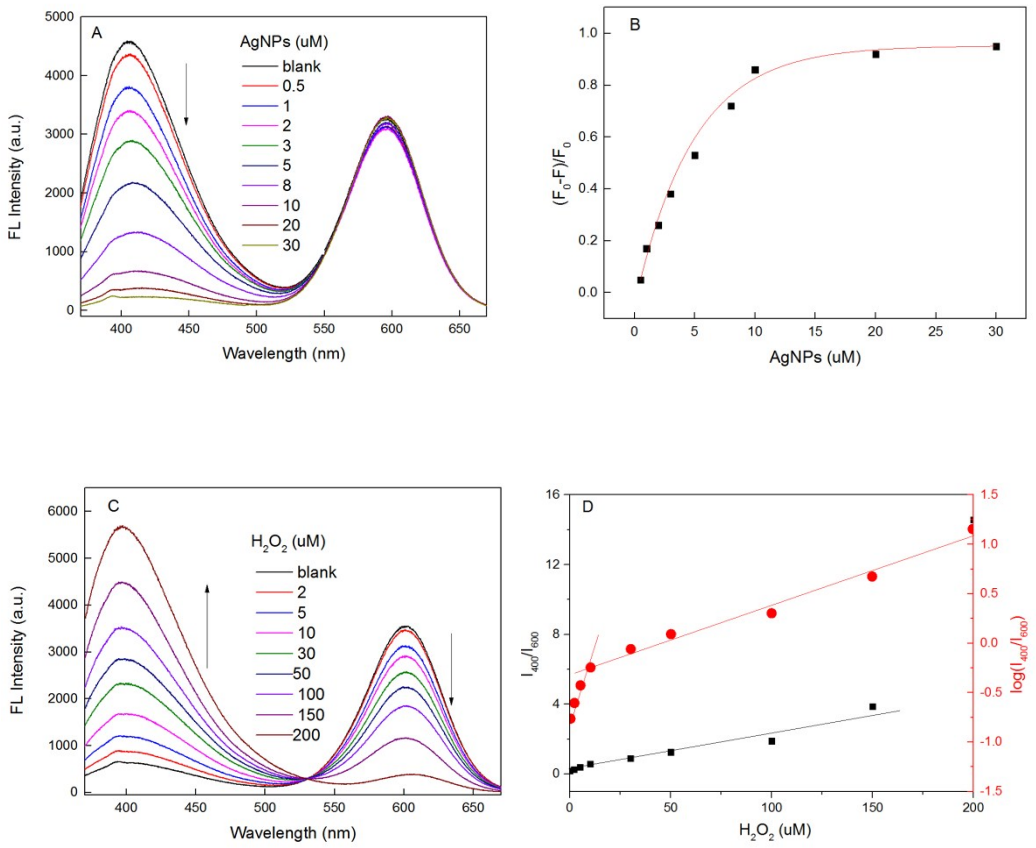

Figure S6 (A) Fluorescence titrations of the D-RFP (100 μg·mL^{-1}) with Ag NPs from 0.5 to 30μM.

(B) Quenching efficiency of D-RFP (100 μg·mL^{-1}) versus the concentration Ag NPs at 400 nm.

(C) Fluorescence response of D-RFP and Ag NPs (100 μg.mL^{-1} and 10 μM, respectively) in the presence of different concentration of H_2O_2.

(D) The relationship between ratio of fluorescence intensity of the D-RFP in (C) versus concentration of H_2O_2.

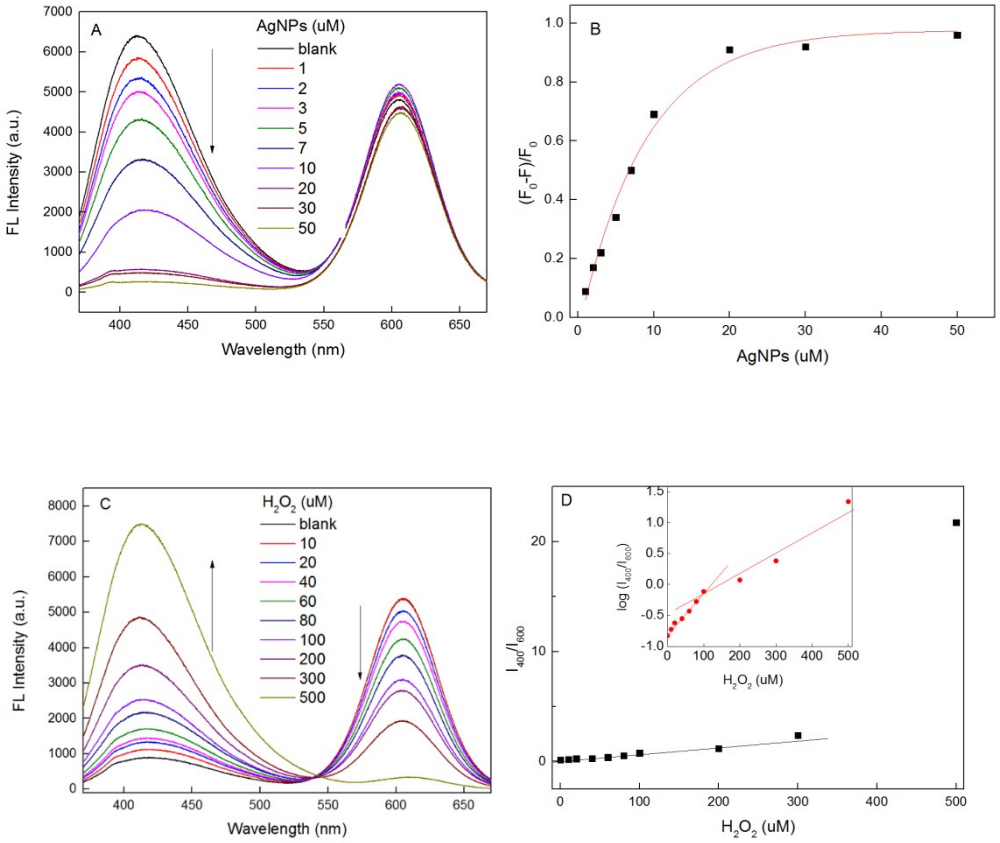

Figure S7 (A) Fluorescence titrations of the D-RFP (150 μg·mL^{-1}) with Ag NPs from 1 to 50 μM.

(B) Quenching efficiency of D-RFP (150 μg·mL^{-1}) versus the concentration Ag NPs at 400 nm.

(C) Fluorescence response of D-RFP and Ag NPs (150 μg.mL^{-1} and 20 μM, respectively) in the presence of different concentration of H_2O_2.

(D) The relationship between ratio of fluorescence intensity of the D-RFP in (C) versus concentration of H_2O_2.

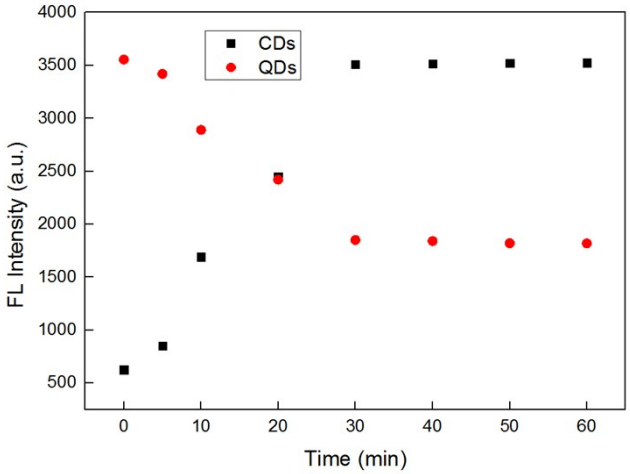

Figure S8 The reaction time on the FL intensity of CDs and QDs.

6. Optimization of reaction conditions for glucose detection

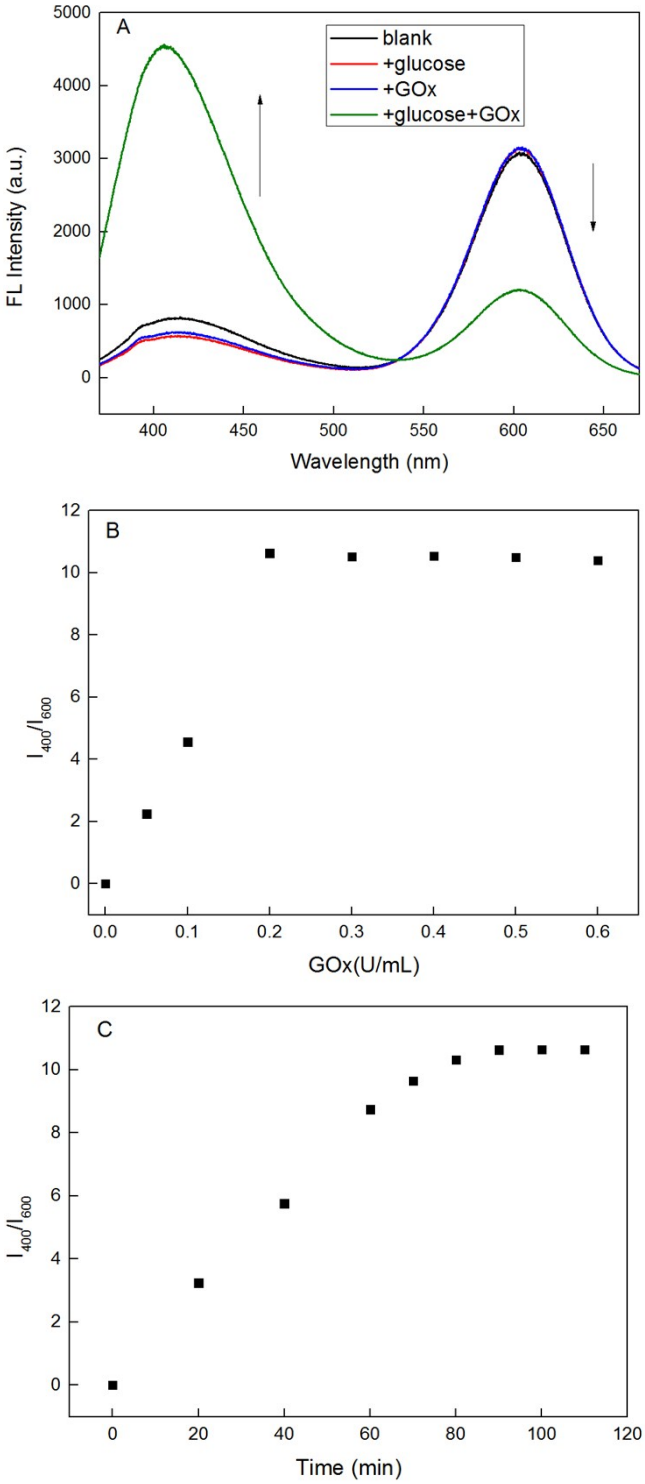

Figure S 9 (A) The florescence spectrum of D-RFP with glucose, GluOx, glucose and GluOx. B） Fluorescence responses of the sensing system toward 500 μM glucose addition at different amount of GluOx. (C) The reaction time of GluOx and glucose on the ratio of FL intensity of D-RFP.

7. Comparison of our method and other fluorescence methods

Table S1 Comparison of sensitivity of our method to other fluorescence methods for glucose detection.

Probe	Method	H_2O_2		Glucose		Reference
		Linear range (μM)	LOD (μM)	Linear range (μM)	LOD (μM)	
Rox-DNA Functionalized CdZnTeS QDs	RFP	0.33-50	0.075	2-100	0.045	1
AgNP-DNA@GQDs Hybrid	Single fluorescent	0.4-200	0.10	2-100	0.42	2
CDs/AgNPs Hybrid	Single fluorescent	10-100	--	2-100	1.39	3
dsDNA-CuNPs and DNA intercalator (SYBR Green I)	RFP	12.5-500	2.6	20-400	8.5	4
DNA-AgNPs/UCNP nanocomposite	Single fluorescent	2-80	1.08	2.5-100	1.41	5
CDs/AgNPs Hybrid	Single fluorescent	1.0-100	--	50-300	1.0	6
perylene probe/ AgNPs Hybrid	Single fluorescent	--	--	0-200	2.5	7
CDs@QDs/ AgNPs Hybrid	RFP	1-150	0.28	2-200	0.59	This work

8. Clinical sample detection

Table S2 The determination of glucose in human serum from diabetics and healthy individuals

Sample	Healthy person (mM)			Diabetes patient (mM)		
	H1	H2	H3	D1	D2	D3
This method	4.2	3.9	4.4	13.2	12.8	14.1
Commercial kit	4.3	3.8	4.4	13.4	12.9	13.9

Table S 3 The recovery of spiked glucose in diluted human serum samples. The standard deviation of each sample was obtained by three measurements

Sample	Detected (μM)	Added (μM)	Detected (μM)	Recovery (%)	RSD (%)
1	19.50.	20.00	40.12	101.5	3.4
2	19.50	50.00	69.24	99.6	2.6
3	19.50	100.00	116.4	97.4	4.7

9. Reference

(1) Mao, G,; Cai, Q,; Wang, F.; Luo, C.; Ji, X.; He, Z.; *Anal. Chem.* **2017**, *89*, 11628-11635.

(2) Wang, Li.; Zheng, J.; Li, Y.; Yang, S.; Liu, C.; Xiao, Y.; Li, J.; Cao, Z.; Yang, R.; *Anal. Chem.* **2014**, *86*, 12348-12354.

(3) Ma, J.; Yin, B.; Wu, X.; Ye, B.; *Anal. Chem.* **2017**, *89*, 1323-1328.

(4) Chen, J.; Ji, X.; He, Z.; *Anal. Chem.* **2017**, *89*, 3988-3995.

(5) Wu, S.; Kong, X.; Cen, Y.; Yuan, J.; Yu, R.; Chu, X.; *Nanoscale* **2016**, *8*, 8939-8946.

(6) Li, H.; Yan, X.; Qiao, S.; Lu, G.; Su, X.; *ACS Appl. Mater. Interfaces* **2018**, *10*, 7737-7744.

(7) Li, J.; Li, Y.; Chen, J.; Chen, Y.; Wang, Y.; Yang, M.; Yu, C.; *Chem. Commun.* **2015**, *51*, 6354-6356.